JOURNAL OF VIROLOGY, June 2002, p. 5759–5768 Vol. 76, No. 11
0022-538X/02/$04.00+0 DOI: 10.1128/JVI.76.11.5759–5768.2002

Retrograde Transport of Transmissible Mink Encephalopathy within Descending Motor Tracts

Jason C. Bartz,[1] Anthony E. Kincaid,[2] and Richard A. Bessen[1]*

Department of Medical Microbiology and Immunology[1] and Department of Physical Therapy,[2] Creighton University, Omaha, Nebraska 68178

Received 10 December 2001/Accepted 5 March 2002

The spread of the abnormal conformation of the prion protein, PrP^{Sc}, within the spinal cord is central to the pathogenesis of transmissible prion diseases, but the mechanism of transport has not been determined. For this report, the route of transport of the HY strain of transmissible mink encephalopathy (TME), a prion disease of mink, in the central nervous system following unilateral inoculation into the sciatic nerves of Syrian hamsters was investigated. PrP^{Sc} was detected at 3 weeks postinfection in the lumbar spinal cord and ascended to the brain at a rate of approximately 3.3 mm per day. At 6 weeks postinfection, PrP^{Sc} was detected in the lateral vestibular nucleus and the interposed nucleus of the cerebellum ipsilateral to the site of sciatic nerve inoculation and in the red nucleus contralateral to HY TME inoculation. At 9 weeks postinfection, PrP^{Sc} was detected in the contralateral hind limb motor cortex and reticular thalamic nucleus. These patterns of PrP^{Sc} brain deposition at various times postinfection were consistent with that of HY TME spread from the sciatic nerve to the lumbar spinal cord followed by transsynaptic spread and retrograde transport to the brain and brain stem along descending spinal tracts (i.e., lateral vestibulospinal, rubrospinal, and corticospinal). The absence of PrP^{Sc} from the spleen suggested that the lymphoreticular system does not play a role in neuroinvasion following sciatic nerve infection. The rapid disease onset following sciatic nerve infection demonstrated that HY TME can spread by retrograde transport along specific descending motor pathways of the spinal cord and, as a result, can initially target brain regions that control vestibular and motor functions. The early clinical symptoms of HY TME infection such as head tremor and ataxia were consistent with neuronal damage to these brain areas.

The transmissible spongiform encephalopathies, or prion diseases, are progressive neurodegenerative diseases of animals and humans. Prion infection by peripheral routes, such as intraperitoneal infection, results in prion replication in the lymphoreticular system (LRS) prior to neuroinvasion of the peripheral and central nervous system (CNS). In natural prion diseases, oral exposure is the likely route of infection in bovine spongiform encephalopathy, transmissible mink encephalopathy (TME), and kuru of humans. Oral transmission is also a possible route of transmission in scrapie of sheep, chronic wasting disease of deer and elk, and variant Creutzfeldt-Jakob disease in humans.

Experimental oral exposure of rodents to scrapie reveals that initial infection is established in the gut-associated lymphoid tissue and autonomic ganglia in the enteric nervous system (5, 37). Spread of the abnormal isoform of the prion protein, PrP^{Sc}, from the gastrointestinal tract proceeds along both the splanchnic nerves to the spinal cord and the vagal nerve to the brainstem (6, 39). Neuroinvasion of the spinal cord from peripheral sites subsequently results in prion transport to the brain (26, 27). The follicular dendritic cell (FDC), located in the germinal center of secondary lymphoid tissues, is the primary location of scrapie replication outside of the nervous system (29, 38). Experimental scrapie infection of mice by the peritoneal route demonstrates that replication of murine scrapie strains ME7 and RML in lymphoid tissue is blocked in knockout mice that do not contain mature FDCs (35). Replication of ME7 scrapie is also blocked in peripheral tissues of chimeric mice that do not express the normal isoform of the prion protein, PrP^{C}, in FDCs (10). In addition, these murine scrapie strains do not replicate in the LRSs of wild-type mice in which FDCs are induced to temporarily undergo dedifferentiation (35, 41).

Neuroinvasion of scrapie following peripheral routes of infection has been established in the absence of LRS infection (16, 36, 44). In one study, peripheral scrapie inoculation was performed in transgenic mice that had restricted expression of Syrian hamster PrP^{C} in a subset of neuronal cells (i.e., cells controlled by the neuron-specific enolase promoter) and no expression of PrP^{C} in FDCs (44). In these mice, scrapie infection was not established in the LRS, but they were susceptible to scrapie by the intraperitoneal and oral routes of inoculation. In addition, these mice, which lacked expression of PrP^{C} on FDCs, had incubation periods similar to those of transgenic mice in which PrP^{C} is expressed in many tissue types, including that of the LRS. Splenectomy, which delays the onset of clinical symptoms in wild-type mice due to the removal of a major LRS replication site, had no effect on the incubation period in transgenic mice with neuron-restricted PrP gene expression following intraperitoneal scrapie inoculation. These findings demonstrate that in the absence of LRS infection, peripheral infection, including oral exposure, can lead to scrapie infection of the CNS and disease (44). The study presented here sup-

* Corresponding author. Mailing address: Department of Medical Microbiology and Immunology, Creighton University, 2500 California Plaza, Omaha, NE 68178. Phone: (402) 280-3072. Fax: (402) 280-1875. E-mail: rbessen@creighton.edu.

ports an alternate or additional pathway of prion infection that is LRS-independent and that most likely results in direct infection of nerves and transport to the CNS.

The transport of prions along neural circuitry has been demonstrated in the retinotectal pathway following unilateral intraocular scrapie inoculation (14, 15). The spread of scrapie infectivity can be traced along the optic nerve and tract to the contralateral superior colliculus and visual cortex. The formation of spongiform lesions in these brain regions is initially asymmetrical but, at later time points, develops ipsilaterally to the site of ocular infection (14, 15). These intraocular inoculation studies demonstrate that scrapie is transported along optic nerve axons and that in this model, distribution of scrapie in the brain initially follows the neural circuitry of the visual system. Since the route of prion transport within the spinal cord has not been established and PrP^{Sc} deposits are found in spinal gray matter (19, 37, 39, 40, 48, 57), the aim of the present study was to investigate the spread of TME from the sciatic nerve to the brain in the Syrian hamster. In addition, we examined the patterns of prion deposition in the spinal cord, brain stem, and cerebrum in order to establish whether prion spread took place by axonal transport in spinal tracts, by cell-to-cell spread within the spinal gray matter, or a combination of both pathways.

MATERIALS AND METHODS

Animal inoculations and tissue collection. All procedures involving animals were approved by the Creighton University Institutional Animal Care and Use Committee and were in compliance with the *Guide for the Care and Use of Laboratory Animals* (42a). Weanling, outbred (LVK/LAK) Syrian golden hamsters (Harlan Sprague Dawley, Indianapolis, Ind.) were intracerebrally or intraperitoneally inoculated with 25 or 100 μl of a 1% (wt/vol) brain homogenate of the HY strain of the TME agent (HY TME), respectively, as previously described (8). For inoculation of the sciatic nerve, minor surgery was performed. Hamsters were anesthetized with isoflurane (Steris Laboratories, Phoenix, Ariz.), and the right sciatic nerve was exposed through an incision in the skin and muscle that was parallel to the femur. The sciatic nerve was grasped with a smooth-tipped forceps and pulled upward by placing an unclasped forceps behind the nerve. A 30-gauge hypodermic needle was inserted through the epineurium of the sciatic nerve, and 5 μl of a 1% (wt/vol) brain homogenate ($10^{5.2}$ 50% lethal doses [LD_{50}]) of HY TME was slowly inoculated (trial 1). To prevent leakage of inocula from the injection site, the needle was slowly withdrawn after 30 to 60 s. In trial 2, following insertion of the needle into the epineurium and prior to inoculation, the 30-gauge needle was moved up and down parallel to the nerve for a distance of several millimeters for 10 consecutive strokes. In both trials, the sciatic nerve was repositioned and surgical staples were used for skin closure. Animals were observed at least three times per week for onset of neurological disease as previously described (8). Hamsters were sacrificed by CO_2 asphyxiation, and tissues (e.g., brain, sciatic nerve, spleen, and spinal cord) were removed for analysis. For intramuscular inoculations, 20 μl of a 1% (wt/vol) brain homogenate of HY TME was injected into the right femoral bicep muscle.

To examine the temporal accumulation of PrP^{Sc} in the spinal cord following sciatic nerve inoculation, three animals were sacrificed each week postinfection for 10 consecutive weeks. The spinal cord was dissected into the following vertebral segments: cervical segments 2 to 4 (C2 to C4) and C5 to C7; thoracic segments 1 to 3 (T1 to T3), T4 to T6, T7 to T9, and T10 to T13; and lumbar segments 1 to 5 (L1 to L5). Spleen and sciatic nerve sections were collected for PrP^{Sc} analysis, and the brain and brain stem were fixed in formalin and processed for PrP^{Sc} immunohistochemistry.

Tissue preparation for PrP^{Sc} Western blotting. For PrP^{Sc} analysis of 0.5-mg tissue equivalents, spinal cord was homogenized to 10% (wt/vol) and an equal volume of phosphate-buffered saline containing 200 μg per ml of proteinase K (PK) (USB Corporation, Cleveland, Ohio) was added. Following incubation at 37°C for 1 h, phenylmethylsulfonyl fluoride was added to a final concentration of 2 mM and samples were analyzed for PrP^{Sc} content by sodium dodecyl sulfate-polyacrylamide gel electrophoresis (SDS-PAGE) and Western blotting. PrP^{Sc} analysis of 20- to 50-mg tissue equivalents was performed by adjusting tissue homogenates (10% [wt/vol] spinal cord, 20% [wt/vol] spleen and sciatic nerve) to 5 mM $MgCl_2$ prior to the addition of 100 U of Benzonase nuclease/ml (Novagen, Inc., Madison, Wis.) and incubation at 37°C for 1 h with constant shaking. An equal volume of buffer A (20% [wt/vol] *N*-lauroylsarcosine in 10 mM Tris-HCl [pH 7.5]) was added, and the sample was continuously vortexed for 30 min at room temperature. Tissue homogenates were subjected to ultracentrifugation at 10,000 × *g* and 10°C for 30 min in a TLA-45 rotor (Beckman Instruments, Palo Alto, Calif.). The supernatant (S1) was collected, and the pellet (P1) was resuspended in half of the original volume of buffer A. The vortex and centrifugation steps were repeated as described above. S2 was collected and combined with S1; this was followed by centrifugation of both supernatants at 200,000 × *g* and 10°C for 60 min in a TLA-45 rotor. The supernatant (S3) was discarded, and the pellet (P3) was resuspended in H_2O (1 μl per mg of original tissue weight) by using a cup horn sonicator (Fisher Scientific, Atlanta, Ga.). PK was added to a final concentration of 10 μg per ml, and the suspension was incubated at 37°C for 30 min with constant shaking. Phenylmethylsulfonyl fluoride was added to reach a concentration of 5 mM followed by centrifugation at 200,000 × *g* and 10°C for 60 min in a TLA-45 rotor. The supernatant (S4) was discarded, and the pellet (P4) was resuspended in SDS-PAGE sample loading buffer.

Western blot analysis. SDS-PAGE and Western blot analysis were performed as previously described except for modifications in the immunodetection method (3). Following incubation with monoclonal 3F4 ascites fluid (a gift of Richard Kascsak, New York State Institute of Mental Health, Staten Island), polyvinylidene difluoride membranes were washed and incubated with goat anti-mouse immunoglobulin G-alkaline phosphatase conjugate (IgG-AP; Promega, Madison, Wis.) at a 1:30,000 dilution in TTBS (10 mM Tris-HCl [pH 7.4], 150 mM NaCl, 0.5% Tween 20) containing 3% bovine serum albumin for 1 h at room temperature. The membranes were washed and developed with enhanced chemifluorescence (ECF) reagent (Amersham Pharmacia Biotech, Piscataway, N.J.) according to the manufacturer's directions and scanned on a Storm PhosphorImager (Molecular Dynamics, Sunnyvale, Calif.). Quantification of PrP^{Sc} bands from Western blots was performed using ImageQuant software. PrP^{Sc} signal volumes were normalized by using the local median function to correct for background and by subtracting the signal volume of an uninfected brain homogenate (0.5-mg equivalents) that was digested with PK as described above. The normalized signal volume of PrP^{Sc} from each spinal cord sample was expressed as a percentage of the normalized signal volume from a control standard, an HY TME-infected hamster brain homogenate (0.5-mg equivalents) digested with PK. Analysis of the relative PrP^{Sc} signals among samples could be performed when data were represented in this manner.

PrP^{Sc} immunohistochemistry. Immunostaining for PrP^{Sc} on brain tissue was performed as previously described (7). Briefly, formalin-fixed, paraffin-embedded tissue sections (7 μm thick) were subjected to antigen retrieval by using hydrolytic autoclaving (1 to 3 mM HCl) and were incubated with anti-PrP monoclonal antibody 3F4 at a 1:2,000 dilution. The ABC-HRP Elite (Vector Laboratories, Burlingame, Calif.) method was used for antibody signal amplification, and visualization was performed using 3-amino-9-ethylcarbazole in 50 mM sodium acetate (pH 5.0) and 0.03% H_2O_2. Brain and brain stem nuclei were identified in adjacent tissue sections stained with cresyl violet by using a camera lucida attached to a light microscope to map the PrP^{Sc} distribution. Hamster (42) and rat (43) brain atlases were used to aid in the identification of brainstem and brain nuclei.

Gross dissection of the spinal cord. To determine the vertebral level that corresponded to the termination of the spinal cord and to the spinal nerves that contribute to the sciatic nerve, dissection was performed as follows. Four male hamsters were deeply anesthetized and transcardially perfused with 100 ml of 0.01 M phosphate-buffered saline followed by 100 ml of 4% paraformaldehyde in 0.1 M sodium phosphate buffer. The animals were decapitated and eviscerated. The vertebral bodies were identified and numbered using the ribs as landmarks. The spinal cord was then exposed by removal of all vertebral laminae. The conus medullaris was identified, and the adjacent vertebral level was noted. The sciatic nerve was identified in the lower extremity and dissected proximally to the location at which the spinal nerves entered the intervertebral foramen. These spinal nerves were then followed proximally in the vertebral canal to the location at which they entered the spinal cord. The adjacent vertebral level was identified for each of the spinal nerves that contribute to the sciatic nerve.

RESULTS

TME infection of the sciatic nerve. The spread of HY TME from the peripheral nerves to the CNS in golden hamsters was

investigated by inoculating the right sciatic nerve with HY TME. In the first trial, all seven intranerve (i.n.)-inoculated hamsters developed HY TME but the times to onset of clinical signs segregated into short and long incubation groups. The first group of hamsters ($n = 4$) had a short incubation period of 73 ± 7 days (mean ± standard error of the mean), and the second group had a long incubation period ($n = 3$), with onset of clinical signs at 143 ± 12 days postinfection (Fig. 1A). Direct inoculation of HY TME into the femoral bicep muscles of six Syrian golden hamsters resulted in an incubation period of 142 ± 14 days ($n = 7$), suggesting that the long incubation time following sciatic nerve inoculation was not due to direct infection of the peripheral nerve but to infection by a route similar to that followed after intramuscular inoculation (Fig. 1A). Since previous studies (25) reported improved efficiency of scrapie infection following crushing of the sciatic nerve, in a second experiment the sciatic nerve was injured by inserting a 30-gauge needle into the epineurium and repeatedly reciprocating the needle immediately prior to i.n. inoculation. In this group, all animals developed clinical signs of HY TME after an incubation period of 68 ± 2 days (Fig. 1B). The incubation period of the short incubation group in trial 1 was not statistically different ($P > 0.1$) from the incubation period in trial 2. Since mild injury to the sciatic nerve prior to HY TME inoculation resulted in a consistent and short incubation period, this method of HY TME i.n. inoculation was used in all subsequent experiments. Using the sciatic nerve injury method of HY TME inoculation, the incubation period was longer than that of intracerebral inoculation (59 ± 2 days; $P < 0.01$) but shorter than that of intraperitoneal (101 ± 2 days; $P < 0.01$) or intramuscular ($P < 0.01$) inoculation (Fig. 1).

Temporal pattern of PrP^{Sc} accumulation in the spinal cord. Gross dissection of the spinal cord determined that the spinal nerves that constitute the sciatic nerve are the fourth through sixth segments of the lumbar spinal cord (L4 to L6). These spinal cord segments anatomically corresponded to thoracic vertebral segments 11 to 13 (T11 to T13). This difference between the spinal cord levels and the vertebral levels is due to the different rates of growth of these two structures. The conus medullaris was located adjacent to vertebral segment L1. Following sciatic nerve inoculation of HY TME, three hamsters were sacrificed every week for 10 consecutive weeks and each spinal cord was dissected into seven parts, each containing three to five vertebral segments.

Western blot analysis was used to investigate the temporal distribution of PrP^{Sc} in the spinal cord. A 5% (wt/vol) spinal cord homogenate (0.5-mg tissue equivalents) was digested with PK (100 μg/ml) prior to Western blotting and quantification of PrP^{Sc} signals. This method only detects PrP^{Sc}, because PrP^{C} was degraded during the PK digestion step (data not shown). Serial dilution of HY TME-infected brain homogenates digested with PK (100 μg per ml) demonstrated that the lower limit of PrP^{Sc} detection in 10 μl of a 5% (wt/vol) homogenate was approximately 100 ng of tissue equivalents (data not shown). This amount of PrP^{Sc} approximately corresponds to $10^{2.8}$ LD_{50}, based on a starting brain titer of $10^{9.5}$ LD_{50} per gram of HY TME (8).

To investigate the temporal deposition of PrP^{Sc} in the spinal cord, the relative amounts of PrP^{Sc} in each vertebral spinal cord segment at each weekly interval were quantified from Western blots and expressed as percentages of the signal intensity of a hamster brain homogenate from a clinical case of HY TME. PrP^{Sc} was first detected in the spinal cord at 4 weeks postinfection in vertebral levels T10 to T13 (Fig. 2A), which

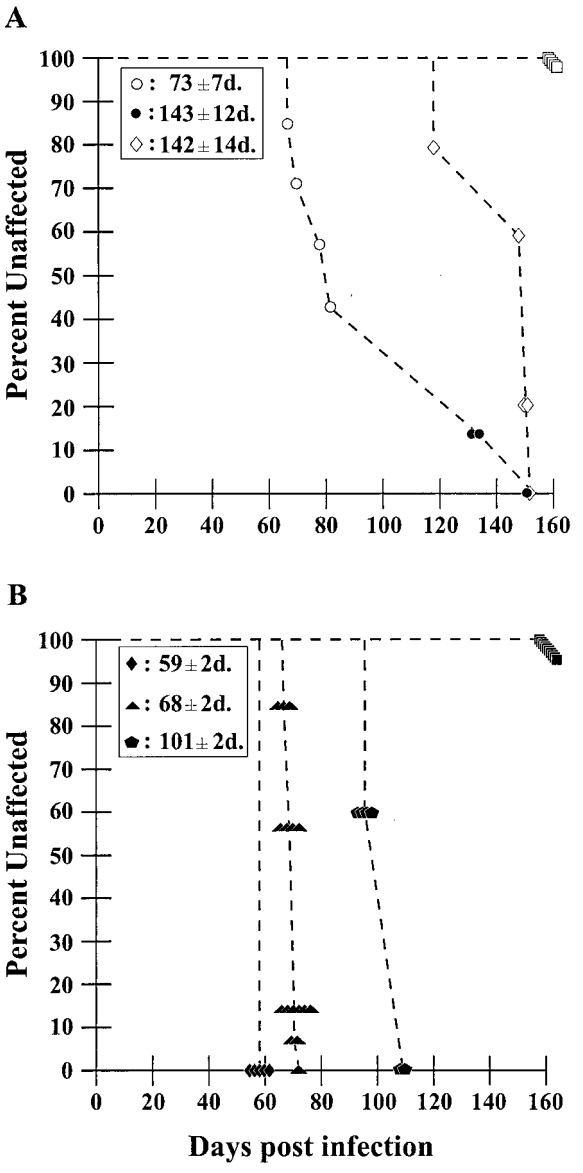

FIG. 1. Incubation period following sciatic nerve inoculation of HY TME. In trial 1 (A), hamsters inoculated in the sciatic nerve with HY TME segregated into short and long incubation groups based on the onset of clinical signs. The short incubation group (open circle; $n = 4$) had an incubation period of 73 ± 7 days, while the long incubation group (filled circle; $n = 3$) had an incubation period of 143 ± 12 days. The incubation period for the latter group was not statistically different ($P > 0.01$) from that for the intramuscularly inoculated hamsters (142 ± 14 days; diamond, $n = 5$). Mock-infected hamsters (open square; $n = 5$) were clinically normal for the duration of the experiment. In trial 2 (B), with use of a modified sciatic nerve inoculation procedure as described in the text, hamsters developed clinical disease at 68 ± 2 days postinfection (filled triangle; $n = 16$). Intracerebral and intraperitoneal inoculation with HY TME resulted in incubation periods of 59 ± 2 days (filled diamond; $n = 5$) and 101 ± 2 days (filled pentagon; $n = 6$), respectively. Mock-infected hamsters were clinically normal for the duration of the experiment (filled square; $n = 9$).

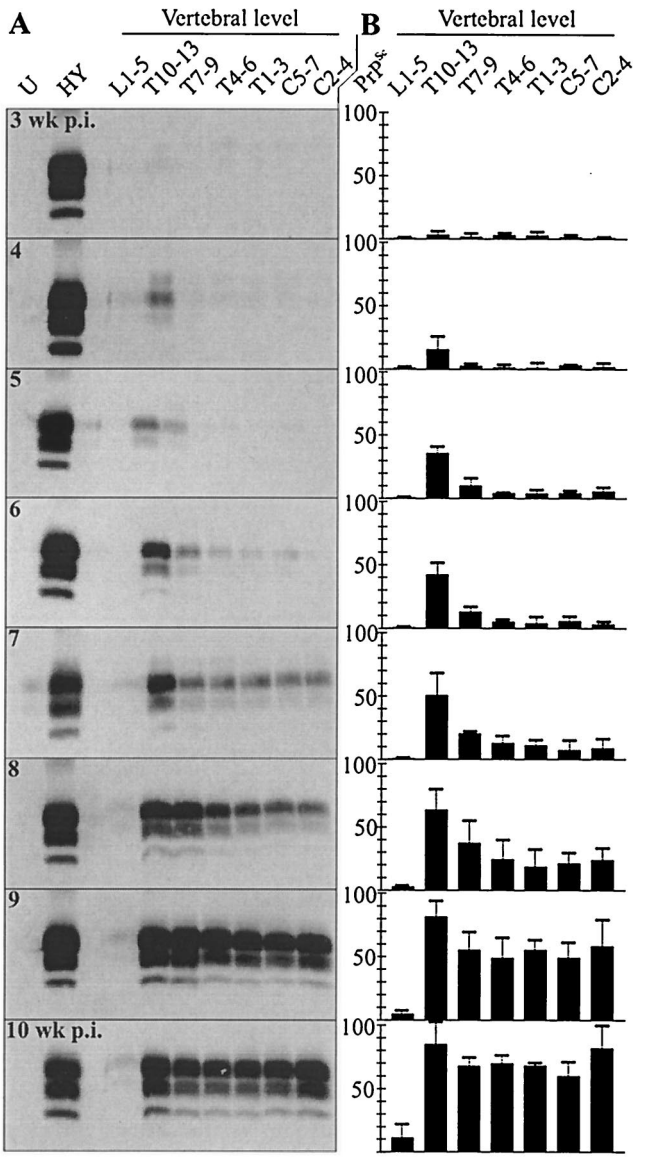

FIG. 2. Temporal distribution of PrP^{Sc} in the spinal cord following sciatic nerve inoculation of HY TME. Western blot analysis (A) and quantification (B) of PrP^{Sc} (0.5-mg tissue equivalent) in spinal cord between 3 and 10 weeks postinfection (p.i.). The relative amount of PrP^{Sc} in each spinal cord segment (indicated as vertebral level) was expressed as a percentage of the PrP^{Sc} signal from a HY TME-infected brain (0.5-mg brain equivalent) at terminal disease. PrP^{Sc} signal was measured using a Storm PhosphorImager and ImageQuant software. Illustrated are Western blots from individual hamsters (A) and the relative PrP^{Sc} signal intensities (PrP^{Sc}) from an average of three animals (B) at each week postinfection. Standard errors are indicated. Spinal cord vertebral segments refer to lumbar (L), thoracic (T), and cervical (C). Uninfected (U) brain homogenate controls are indicated.

include the spinal cord segments (L4 to L6) that give rise to the sciatic nerve. PrP^{Sc} was detected in vertebral segments T7 to T9 at 5 weeks postinfection, and for these first two time points there appeared to be a front edge of PrP^{Sc} that spread in a rostral direction along the spinal cord. Between 6 and 7 weeks postinfection, PrP^{Sc} was found in the remaining levels of the thoracic spinal cord and in the cervical spinal cord (Fig. 2A). The amount of PrP^{Sc} in the spinal cord steadily increased during the course of HY TME infection without reaching a plateau (Fig. 2B). For each week between 4 and 8 weeks postinfection, the amount of PrP^{Sc} was highest in vertebral levels T10 to T13 and the amount of PrP^{Sc} declined in each consecutive spinal cord segment until reaching the mid-cervical spinal cord (Fig. 2B). These findings suggest that upon entering the lumbar spinal cord, HY TME replicated and spread in a caudal-to-rostral direction along the spinal cord. When clinical signs first appeared at 10 weeks postinfection, PrP^{Sc} levels were at least 60% of that of the HY TME brain control (Fig. 2B). PrP^{Sc} accumulation in lumbar vertebral segments L1 to L5 was approximately 10% of that of the HY TME brain control at 10 weeks postinfection, but tissue taken at this vertebral segment contained the spinal nerves and not the spinal cord, as the spinal cord ends at L1. Similar results were obtained for all three animals at each of the weekly time points (Fig. 2B and data not shown).

Rate of PrP^{Sc} spread in the nervous system. The rate of PrP^{Sc} spread from the site of sciatic nerve inoculation to the CNS was investigated by measuring the earliest time point at which PrP^{Sc} was detected by Western blot analysis in the caudal and rostral vertebral segments of the spinal cord, specifically in T10 to T13 and C2 to C4. In these experiments, more than 40 times the amount of tissue was analyzed for PrP^{Sc} content as was analyzed in the experiment whose results are depicted in Fig. 2. Partial purification of PrP^{Sc} from 20- to 25-mg tissue equivalents of each spinal cord segment, or more than 90% of each segment, was performed prior to Western blotting. In vertebral levels T10 to T13 and C2 to C4, PrP^{Sc} was first detected at 3 weeks and 5 weeks postinfection, respectively (Fig. 3), which was 1 to 2 weeks prior to detection of PrP^{Sc} in brain homogenates containing 0.5-mg tissue equivalents (Fig. 2). The distance from the midpoint of T10 to T13 to the midpoint of C2 to C4 was approximately 46 mm, which corresponded to a rate of PrP^{Sc} spread of 3.3 mm per day.

Peripheral sites of PrP^{Sc} deposition. To determine whether HY TME established infection in the LRS following sciatic nerve inoculation, the presence of PrP^{Sc} in the spleen was investigated. Western blot analysis was unable to detect PrP^{Sc}

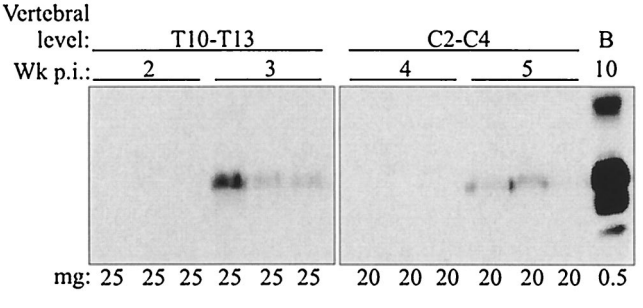

FIG. 3. Western blot analysis of spinal cord segments enriched for PrP^{Sc} after sciatic nerve infection with HY TME. Thoracic (T) and cervical (C) spinal cord homogenates were enriched for PrP^{Sc} by detergent extraction and PK digestion as described in Materials and Methods and analyzed by Western blotting for PrP^{Sc} levels at the indicated intervals postinfection (Wk p.i.). The amounts in milligrams (mg) of tissue equivalents that were analyzed are indicated for each lane. Brain (B) homogenates from HY TME-infected hamsters with clinical symptoms were prepared as described for Fig. 2.

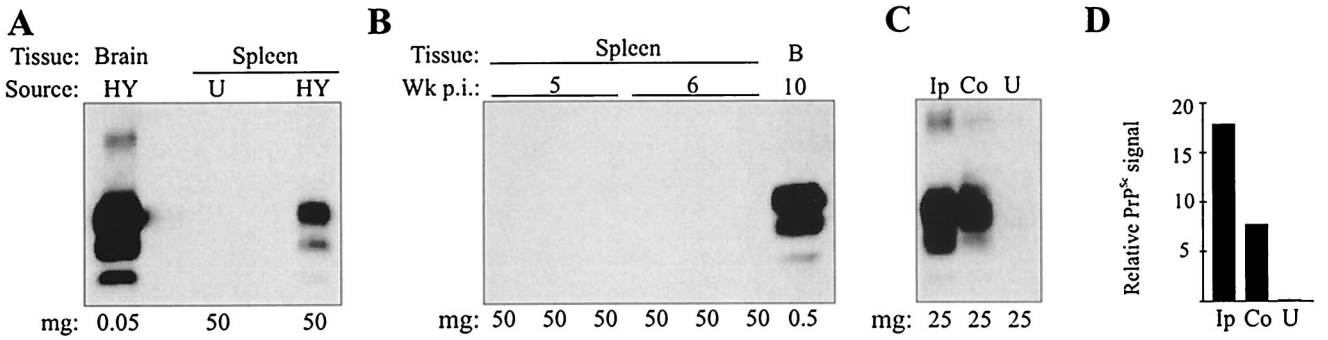

FIG. 4. Immunodetection of PrP^{Sc} in spleen and sciatic nerve after infection with HY TME. (A) Western blot analysis of spleen from uninfected (U) and HY TME-infected hamsters following intracerebral inoculation. Spleens were prepared for analysis as described for spinal cord homogenates in Fig. 3. (B) Western blot analysis of spleen at 5 and 6 weeks postinfection from hamsters inoculated in the sciatic nerve with HY TME. A control HY TME-infected brain (lane B) was prepared as described for Fig. 2. Western blot analysis (C) and PhosphorImager and ImageQuant quantification (D) of PrP^{Sc} in the sciatic nerve at 10 weeks postinfection. Hamsters were inoculated in the sciatic nerve with HY TME and the ipsilateral (Ip), contralateral (Co), and uninfected (U) sciatic nerves were removed and prepared for Western blot analysis as described for spinal cord homogenates in Fig. 3. The amounts in milligrams (mg) of tissue equivalents that were analyzed are indicated for each lane.

in a PrP^{Sc}-enriched spleen preparation containing 50-mg tissue equivalents (i.e., approximately 50% of the total spleen weight) from 1 to 6 weeks postinfection (Fig. 4A and B). Since PrP^{Sc} was detected at 5 weeks postinfection in C2 to C4 (20-mg equivalents) following i.n. inoculation (Fig. 3), the absence of PrP^{Sc} from the spleen at 6 weeks postinfection suggests that PrP^{Sc} deposition in the spinal cord was not due to HY TME neuroinvasion of the thoracic spinal cord following establishment of HY TME infection in the spleen or LRS.

Following sciatic nerve inoculation of HY TME, deposition of PrP^{Sc} in the sciatic nerve (25-mg tissue equivalents) was not detected until 9 weeks postinfection. The amount of PrP^{Sc} in the ipsilateral sciatic nerve was greater than that in the contralateral sciatic nerve at 10 weeks postinfection (Fig. 4C and D). These results suggested that the sciatic nerve was primarily involved in transport of HY TME to the spinal cord, possibly via axonal transport, but was not a major site of HY TME replication.

Spatial distribution of PrP^{Sc} in the brain and brain stem. The anatomical location of PrP^{Sc} in the brain was investigated in order to identify the structures involved in the accumulation and transport of HY TME within the CNS. PrP^{Sc} was first identified at 6 weeks postinfection in the red nucleus, lateral vestibular nucleus (LVe), and interposed nucleus of the cerebellum (Table 1); these structures are involved in the control of motor functions, including balance and coordination. The results of PrP^{Sc} immunostaining with respect to general appearance were similar for all of these areas during the following weeks. Initially, PrP^{Sc} deposition was only found on one side of the brain or brain stem. At 8 weeks postinfection, PrP^{Sc} deposits had a bilateral distribution but more intense PrP^{Sc} immunostaining was found on the side in which PrP^{Sc} was initially detected. At 10 weeks postinfection, PrP^{Sc} deposition had spread beyond the initial sites of deposition in the brain stem but deposits in the cerebral cortex maintained a restricted distribution that did not extend beyond the initial PrP^{Sc} pattern.

Initially, PrP^{Sc} deposits were detected in the red nucleus on the side of the brain contralateral to the site of HY TME inoculation (Table 1), but by 10 weeks postinfection, strong PrP^{Sc} immunostaining was found in both the contralateral and ipsilateral red nuclei (Fig. 5A). PrP^{Sc} deposits were more intense in the ventral and ventrolateral portions of the red nucleus (Fig. 5A and B), which are the areas known to contain neurons that project to the lumbar spinal cord (46, 47). PrP^{Sc} deposits appeared to be localized within the soma of neurons in the red nucleus in some cases, but often it was not possible to determine whether PrP^{Sc} was extracellular or present within axons or dendrites. The intense PrP^{Sc} staining pattern in the ventral portion of the red nucleus was accompanied by prominent spongiform lesions (Fig. 5C). The initial distribution of PrP^{Sc} was consistent with HY TME transport from the ipsilateral lumbar spinal cord to the contralateral red nucleus via the rubrospinal tract, since the rubrospinal fibers cross midline in the ventral tegmental decussation.

At 6 weeks postinfection, PrP^{Sc} deposition in the LVe and the interposed nucleus of the cerebellum was ipsilateral to the site of sciatic nerve inoculation (Table 1 and Fig. 6A and D). At later time points, PrP^{Sc} was identified in both the ipsilateral and contralateral LVe and the interposed nuclei (Table 1).

TABLE 1. Spatial and temporal distribution of PrP^{Sc} following sciatic nerve inoculation with HY TME

CNS region	Wk postinfection[a]					
	5	6	7[e]	8	9[e]	10
Cerebellum-pons						
Lateral vestibular nucleus	0	+[b]	nd	++	nd	++++
Interposed nucleus	0	+[b]	nd	++	nd	++++
Mesencephalon						
Red nucleus	0	+[c]	nd	++	nd	++++
Telecephalon						
Hindlimb cortex	0	0	0	+[c,d]	+	++
Diencephalon						
Reticular thalamic nucleus	0	0	0	0	+[c]	++
Ventroposterior thalamic nucleus	0	0	0	0	0	+[c]

[a] Relative intensities of PrP^{Sc} immunostaining: 0, none; +, rare; ++, weak; +++, moderate; ++++, heavy.
[b] Asymmetrical staining pattern ipsilateral to inoculation site.
[c] Asymmetrical staining pattern contralateral to inoculation site.
[d] Result is for one of three animals.
[e] nd, not done.

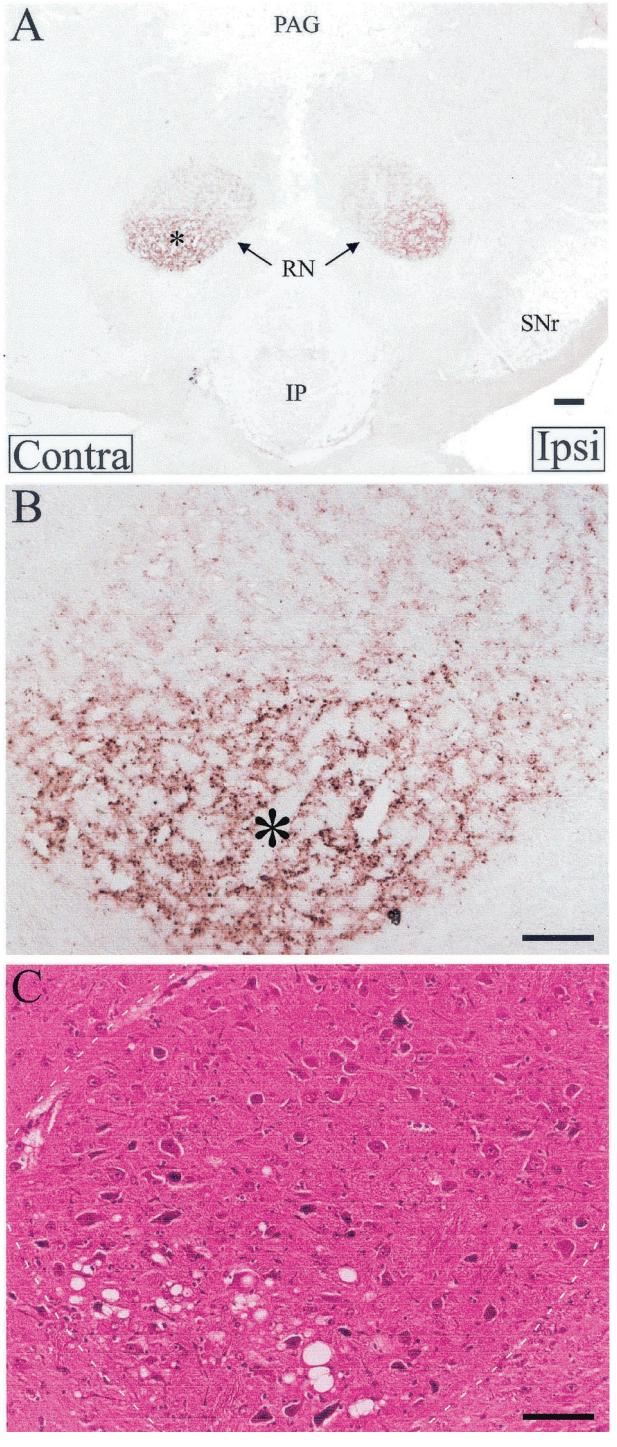

FIG. 5. PrP^{Sc} deposition in the midbrain following HY TME inoculation of the sciatic nerve. (A) PrP^{Sc} immunohistochemistry indicates the location of PrP^{Sc} (red deposits) at 10 weeks postinfection in both red nuclei (RN). The red nucleus located contralateral (asterisk) to sciatic nerve inoculation was viewed at higher magnification using differential interference contrast microscopy (B) to illustrate PrP^{Sc} deposition in the ventral and ventrolateral (asterisk) areas of the red nucleus. (C) Hematoxylin-eosin staining of an adjacent brain section illustrates spongiform lesions in the same area of the red nucleus. Abbreviations: Contra, contralateral; Ipsi, ipsilateral; PAG, periaqueductal gray matter; IP, interpeduncular nucleus; SNr, substantia nigra par reticulata. Bar, 100 micrometers.

PrP^{Sc} deposition in the ipsilateral LVe was consistent with retrograde transport of HY TME in the lateral vestibulospinal tract, since these neurons project their axons to the ipsilateral spinal cord, including the lumbar region (32, 45).

Beginning at 8 to 9 weeks postinfection, PrP^{Sc} deposits were identified in layer V of the contralateral hind limb motor cortex (Table 1 and Fig. 6B, C, E, and F). At later time points, PrP^{Sc} deposits were detected in the ipsilateral motor cortex and the subependymal cell layer that lies dorsal to the labeled area of the motor cortex. This pattern of PrP^{Sc} immunostaining was consistent with retrograde HY TME transport from the ipsilateral lumbar spinal cord to the contralateral hindlimb motor cortex via transport along the descending corticospinal tract (30, 56).

PrP^{Sc} deposition in the thalamus is a prominent feature in hamsters following intracerebral inoculation with the 263K scrapie strain (22, 49) and HY TME (7) but was found to be restricted following sciatic nerve inoculation of HY TME. At 9 to 10 weeks postinfection, only weak PrP^{Sc} immunostaining was detected in the reticular thalamic nucleus that was contralateral to the site of HY TME inoculation. Low levels of PrP^{Sc} immunostaining were occasionally found in the contralateral ventroposterior thalamic nucleus (Table 1).

DISCUSSION

TME infection of the sciatic nerve resulted in the shortest incubation period reported for a peripheral route of prion infection in the Syrian golden hamster. Our findings indicate that sciatic nerve inoculation resulted in HY TME transport to the lumbar spinal cord, subsequent transneuronal spread to spinal tracts that terminate in the lumbar spinal cord, and then retrograde axonal transport to nuclei in the brain and brain stem. The specific targeting of HY TME and spongiform lesions to brain nuclei that have a functional role in coordination, balance, and hind limb motor activity could account for the early onset of clinical signs, which are symptomatic of deficits in these structures, following sciatic nerve inoculation. This is in contrast to the effects of intraocular inoculation, which also establishes direct nerve infection but does not result in short incubation periods in either murine (15) or hamster (11, 28) models compared to the incubation periods for other routes of peripheral inoculation (28). Previous studies using a sciatic nerve model for scrapie infection in mice also resulted in a rapid disease onset that was dependent on either nerve injury (25) or overexpression of the prion protein gene (17).

The PrP^{Sc} deposition pattern in the brain and brain stem indicates that movement of HY TME within the spinal cord involved retrograde transport in the descending lateral vestibulospinal, rubrospinal, and corticospinal tracts. This finding was supported by the initial distribution of HY PrP^{Sc} in the LVe, red nucleus, and motor cortex, respectively. The asymmetrical deposition pattern of PrP^{Sc} in these brain nuclei can be explained by direct axonal transport along spinal tracts that terminate in the lumbar spinal cord and are either predominantly ipsilateral (e.g., lateral vestibulospinal tract) or contralateral (e.g., rubrospinal and corticospinal tracts) to the site of sciatic nerve inoculation (2, 30, 32, 46, 56). The 1- to 2-week delay in the appearance of PrP^{Sc} deposits contralateral to the initial sites of detection could be due to HY TME spread from

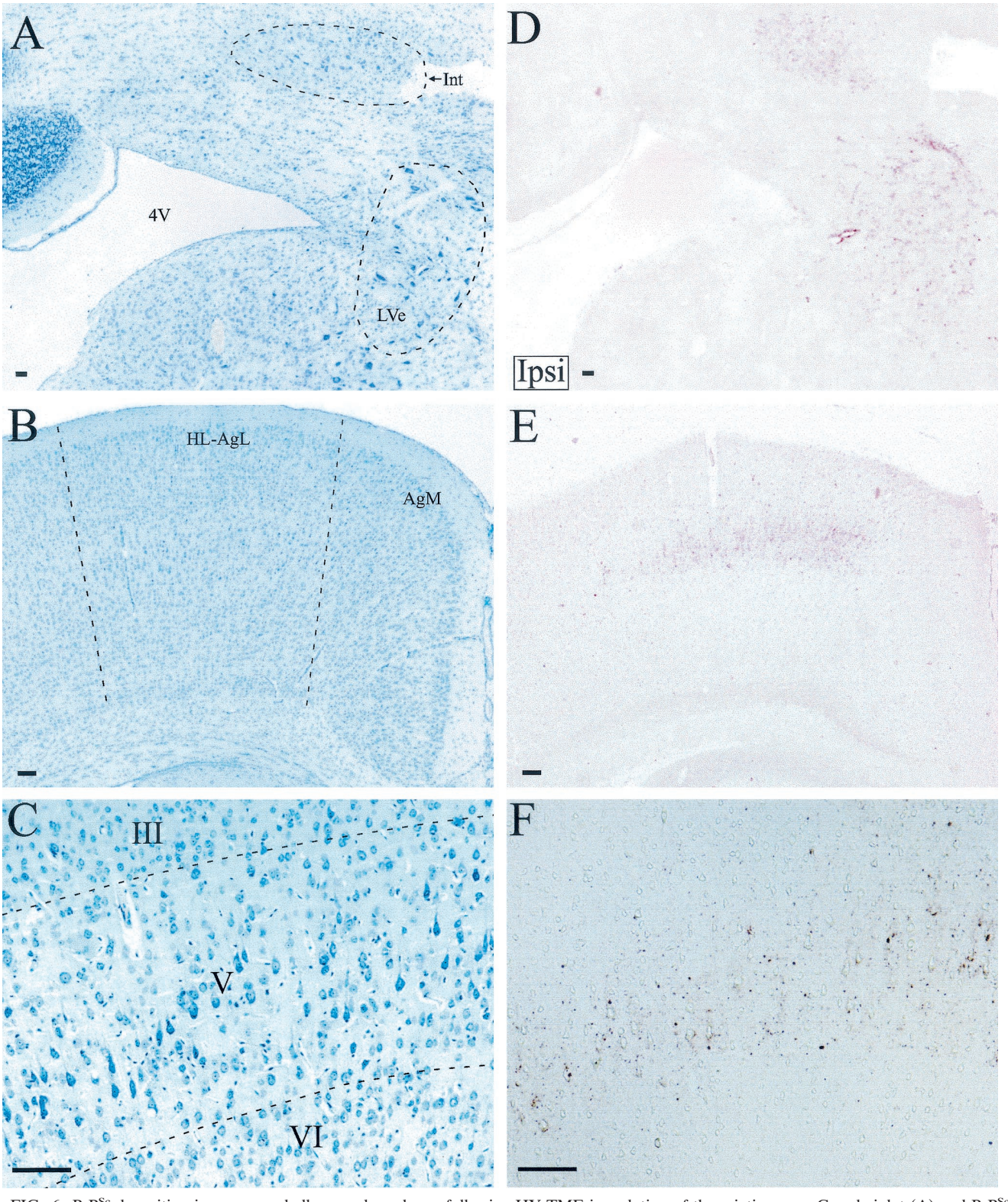

FIG. 6. PrP^{Sc} deposition in pons, cerebellum, and cerebrum following HY TME inoculation of the sciatic nerve. Cresyl violet (A) and PrP^{Sc} immunostaining (red deposits) (D) of the ipsilateral (Ipsi) cerebellum and pons in adjacent brain sections at 8 weeks postinfection, demonstrating the distribution of PrP^{Sc} in the interposed nucleus of the cerebellum (Int) and lateral vestibular nucleus (LVe), is shown. Cresyl violet (B) and PrP^{Sc} immunostaining (E) of the contralateral (Contra) hind limb motor cortex in adjacent brain sections at 9 weeks postinfection, demonstrating the PrP^{Sc} distribution, is shown. (F) Higher magnification from a different brain section illustrates PrP^{Sc} immunostaining in the hind limb motor cortex with respect to the third (III), fifth (V), and sixth (VI) cortical cell layers as viewed by differential interference contrast microscopy. An adjacent cresyl violet-stained brain section is illustrated (C). Abbreviations: 4V, fourth ventricle; HL-AgL, hind limb and lateral agranular cortex; AgM, medial agranular cortex. Bar, 100 micrometers.

the ipsilateral to the contralateral lumbar spinal cord or, more likely, to retrograde transport via the modest ipsilateral rubrospinal and corticospinal tracts and contralateral lateral vestibulospinal tract (2, 30, 32, 46, 56). The selective deposition of PrP^{Sc} in the ventral and ventrolateral half of the red nucleus and in layer V of the hind limb motor cortex following sciatic nerve inoculation is consistent with the previously described somatotopic organization of these descending motor tracts (30, 46, 47, 56).

Since there are no known direct spinal projections from the interposed nucleus of the cerebellum to the spinal cord, we propose that HY TME transport to the interposed nuclei was along collaterals of the descending rubrospinal tract. In the rat, approximately one-third of the rubrospinal neurons have collaterals that project to the interposed nucleus of the cerebellum (21). It is possible that HY TME retrograde transport along the rubrospinal tract resulted in HY TME spread to the contralateral red nucleus as well as anterograde spread to the ipsilateral interposed nucleus via axon collaterals. This type of combined retrograde-anterograde collateral axonal transport has been demonstrated in the cerebellum by using tract tracers (12). The hypothesis of this proposed route of HY TME transport to the interposed nucleus is supported by PrP^{Sc} deposition in these nuclei at the same time as or before accumulation in other brain structures and by the simultaneous appearance of PrP^{Sc} in the interposed nucleus and red nucleus at 6 weeks postinfection. Taken together, these findings suggest that the early presence of PrP^{Sc} in the interposed nucleus was not due to HY TME transport from a synaptically linked brain structure but was most likely due to transport along spinal tracts that terminate in the lumbar spinal cord.

The distribution of PrP^{Sc} in the CNS following sciatic nerve inoculation of HY TME was similar to that reported following the injection of herpes simplex virus type 1 into the tibial nerve, a branch of the sciatic nerve (52). Herpes simplex virus type 1 was detected in layer V of the contralateral hind limb cortex, the ventral part of the contralateral red nucleus, and in hypothalamic nuclei. This distribution is similar to what we report for the present study for HY PrP^{Sc} with the exception of that for the hypothalamus, which showed no evidence of PrP^{Sc} deposition as late as 10 weeks postinfection. In related studies, injection of pseudorabies into either the medial gastrocnemius muscle or the sciatic nerve resulted in prominent retrograde labeling in brain areas involved in autonomic function while sparse labeling was found in areas involved in motor control (23). Therefore, different alphaherpesviruses can be preferentially transported to neuronal structures that appear to be functionally related. A similar phenomenon could be involved in the transport of different strains of prions to distinct regions of the CNS. In a recent study, sciatic nerve inoculation of murine RML scrapie was reported to result in selective targeting of PrP^{Sc} to brain regions involved in sensory function, although the spinal tracts possibly involved in the transport of scrapie were not identified (17). In the present study, HY TME was preferentially targeted to motor structures via descending spinal tracts. Strain-specific targeting of prions could be related to the ability of prion strains to discriminate between functionally distinct nerve terminals and to undergo axonal transport within different spinal tracts.

PrP^{Sc} initially entered the spinal cord in the lumbar region and spread along the spinal cord towards the brain stem at a rate of 3.3 mm per day following sciatic nerve inoculation of HY TME. Previous studies reported the rate of spread for scrapie infectivity and PrP^{Sc} along the spinal cord to be approximately 1.0 mm per day (range, 0.5 to 2.0 mm per day), which is consistent with slow anterograde axonal transport (4, 17, 27). The directional spread of scrapie within spinal tracts was not determined in these reports. In our study, neuroanatomical mapping of PrP^{Sc} deposition strongly suggested that HY TME spreads by retrograde axonal transport in the rubrospinal, vestibulospinal, and corticospinal tracts. However, the rate of spread of HY TME is slower than that of retrograde axonal transport (i.e., approximately 85 mm to 430 mm per day) (18). Several herpesviruses can spread at the rate of fast axonal transport in the anterograde and/or retrograde directions (13, 33, 58), but other viruses that spread by fast axonal transport have measured rates of spread that are below 50 mm per day in some studies. For example, rabies virus has been reported to spread in neuronal processes towards the perikaryon at rates as low as 12 mm per day both in vitro and in vivo (31, 34) and as high as 120 to 400 mm per day along peripheral nerves of rodents (50). Similarly, reoviruses, which are reported to spread in the murine peripheral nervous system by retrograde axonal transport, travel at $\geq$14 mm per day in the sciatic nerve (51). Therefore, the calculated rates of spread for viruses as well as HY TME do not necessarily correspond to the known rates of fast and slow axonal transport. When calculating the distance a virus travels in a given time, it is difficult to separate the actual time involved in axonal transport from that of other viral or prion activities in the cell. In the present study, we measured the times of the initial appearances of HY TME at opposite ends of the spinal cord in order to calculate the rate of spread, but events unrelated to transport (e.g., PrP^{Sc} binding to the cell surface, uptake into the neuron, and/or new PrP^{Sc} formation) may also be required. Additional studies are needed to determine how prions enter neurons and are transported within axons.

The PrP^{Sc} accumulation pattern that formed following intranerve HY TME infection indicated that the sciatic nerve was primarily involved in transport of HY TME along axons, while in the spinal cord there was evidence for both transport along spinal tracts and HY TME replication in spinal gray matter (data not shown). In the peripheral nervous system, we were unable to detect PrP^{Sc} in the sciatic nerve until 9 weeks postinfection despite PrP^{Sc} detection at 3 weeks postinfection in the caudal spinal cord. Our findings suggest that HY TME is transported along the sciatic nerve to the spinal cord with minimal replication, but upon deposition in nerve cell bodies in the spinal cord gray matter, HY TME is able to replicate to high levels. Previous studies have also found higher levels of scrapie infectivity in the spinal cord than in the sciatic nerve at various time points following sciatic nerve inoculation (17, 25). Once HY TME replication begins in the spinal cord, anterograde HY TME transport back to the sciatic nerve could result in accumulation of HY TME infectivity and PrP^{Sc} in peripheral nerves during the later stages of infection. The hypothesis regarding this route of HY TME spread is supported by the presence of twice as much PrP^{Sc} in the HY TME-inoculated sciatic nerve as in the contralateral sciatic nerve. Previous studies have also demonstrated that scrapie infection can

spread from the thoracic spinal cord to thoracic spinal nerves (24).

The short incubation period following sciatic nerve inoculation was likely due to direct nerve infection and was not dependent on HY TME amplification in the LRS prior to neuroinvasion. This hypothesis is supported by the absence of PrP^{Sc} in the spleen at 6 weeks postinfection, at a time when PrP^{Sc} was present in the brain. This conclusion is supported by previous studies in which scrapie inoculation into the sciatic nerve and anterior chamber of the eye did not result in the presence of PrP^{Sc} in the spleen (17) or scrapie infection in the spleen until the late stages of disease (28). These findings raise the possibility that direct infection of the nervous system could be an alternative route of neuroinvasion in natural prion diseases. Support for this hypothesis is provided in findings for experimental murine scrapie in which transgenic mice, whose PrP^{C} expression is restricted to the nervous system, are susceptible to peripheral routes of scrapie infection, including oral exposure. In prion diseases of livestock, the striking paucity of prions in the LRS of bovine spongiform encephalopathy-infected cattle (9, 55) compared to the amounts present in the LRS of scrapie-infected sheep (1, 20, 53, 54) could indicate that bovine spongiform encephalopathy infection of the CNS is independent of LRS infection. Direct infection of the nervous system would be the most likely alternative route in these cases.

ACKNOWLEDGMENTS

This work was supported by a U.S. Department of Agriculture grant (98352046409) and Public Health Service grants awarded by the National Institute of Neurological Diseases and Stroke (5R29NS37914-01) and the NIH National Center for Research Resources (1P20RR15635-01). This work was also supported through the Nebraska Center for Virology. Additional support was provided through a postdoctoral fellowship (to J.C.B.) from USDA/CREES/NRICP (00352049228).

We thank Lauren Heystek and Theresa Bikram Murphy for excellent technical assistance.

REFERENCES

1. **Andreoletti, O., P. Berthon, D. Marc, P. Sarradin, J. Grosclaude, L. van Keulen, F. Schelcher, J. M. Elsen, and F. Lantier.** 2000. Early accumulation of PrP^{Sc} in gut-associated lymphoid and nervous tissues of susceptible sheep from a Romanov flock with natural scrapie. J. Gen. Virol. **81:**3115–3126.
2. **Antal, M., G. N. Sholomenko, A. K. Moschovakis, J. Storm-Mathisen, C. W. Heizmann, and W. Hunziker.** 1992. The termination pattern and postsynaptic targets of rubrospinal fibers in the rat spinal cord: a light and electron microscopic study. J. Comp. Neurol. **325:**22–37.
3. **Bartz, J. C., R. A. Bessen, D. McKenzie, R. F. Marsh, and J. M. Aiken.** 2000. Adaptation and selection of prion protein strain conformations following interspecies transmission of transmissible mink encephalopathy. J. Virol. **74:**5542–5547.
4. **Beekes, M., E. Baldauf, and H. Diringer.** 1996. Sequential appearance and accumulation of pathognomonic markers in the central nervous system of hamsters orally infected with scrapie. J. Gen. Virol. **77:**1925–1934.
5. **Beekes, M., and P. A. McBride.** 2000. Early accumulation of pathological PrP in the enteric nervous system and gut-associated lymphoid tissue of hamsters orally infected with scrapie. Neurosci. Lett. **278:**181–184.
6. **Beekes, M., P. A. McBride, and E. Baldauf.** 1998. Cerebral targeting indicates vagal spread of infection in hamsters fed with scrapie. J. Gen. Virol. **79:**601–607.
7. **Bessen, R. A., and R. F. Marsh.** 1994. Distinct PrP properties suggest the molecular basis of strain variation in transmissible mink encephalopathy. J. Virol. **68:**7859–7868.
8. **Bessen, R. A., and R. F. Marsh.** 1992. Identification of two biologically distinct strains of transmissible mink encephalopathy in hamsters. J. Gen. Virol. **73:**329–334.
9. **Bradley, R.** 1999. BSE transmission studies with particular reference to blood. Dev. Biol. Stand. **99:**35–40.
10. **Brown, K. L., K. Stewart, D. L. Ritchie, N. A. Mabbott, A. Williams, H. Fraser, W. I. Morrison, and M. E. Bruce.** 1999. Scrapie replication in lymphoid tissues depends on prion protein-expressing follicular dendritic cells. Nat. Med. **5:**1308–1312.
11. **Buyukmihci, N., F. Goehring-Harmon, and R. F. Marsh.** 1983. Neural pathogenesis of experimental scrapie after intraocular inoculation of hamsters. Exp. Neurol. **81:**396–406.
12. **Chen, S., and G. Aston-Jones.** 1998. Axonal collateral-collateral transport of tract tracers in brain neurons: false anterograde labeling and useful tool. Neuroscience **82:**1151–1163.
13. **Cook, M. L., and J. G. Stevens.** 1973. Pathogenesis of herpetic neuritis and ganglionitis in mice: evidence of intra-axonal transport of infection. Infect. Immunol. **7:**272–288.
14. **Fraser, H.** 1982. Neuronal spread of scrapie agent and targeting of lesions within the retino-tectal pathway. Nature **295:**149–150.
15. **Fraser, H., and A. G. Dickinson.** 1985. Targeting of scrapie lesions and spread of agent via the retino-tectal projection. Brain Res. **346:**32–41.
16. **Frigg, R., M. A. Klein, I. Hegyi, R. M. Zinkernagel, and A. Aguzzi.** 1999. Scrapie pathogenesis in subclinically infected B-cell-deficient mice. J. Virol. **73:**9584–9588.
17. **Glatzel, M., and A. Aguzzi.** 2000. PrP(C) expression in the peripheral nervous system is a determinant of prion neuroinvasion. J. Gen. Virol. **81:**2813–2821.
18. **Goldstein, L. S., and Z. Yang.** 2000. Microtubule-based transport systems in neurons: the roles of kinesins and dyneins. Annu. Rev. Neurosci. **23:**39–71.
19. **Goodbrand, I. A., J. W. Ironside, D. Nicolson, and J. E. Bell.** 1995. Prion protein accumulation in the spinal cords of patients with sporadic and growth hormone associated Creutzfeldt-Jakob disease. Neurosci. Lett. **183:**127–130.
20. **Heggebo, R., C. M. Press, G. Gunnes, K. I. Lie, M. A. Tranulis, M. Ulvund, M. H. Groschup, and T. Landsverk.** 2000. Distribution of prion protein in the ileal Peyer's patch of scrapie-free lambs and lambs naturally and experimentally exposed to the scrapie agent. J. Gen. Virol. **81:**2327–2337.
21. **Huisman, A. M., H. G. J. M. Kuypers, F. Conde, and K. Keizer.** 1983. Collaterals of rubrospinal neurons to the cerebellum in rat. A retrograde fluorescent double labeling study. Brain Res. **264:**181–196.
22. **Jendroska, K., F. P. Heinzel, M. Torchia, L. Stowring, H. A. Kretzschmar, A. Kon, A. Stern, S. B. Prusiner, and S. J. DeArmond.** 1991. Proteinase-resistant prion protein accumulation in Syrian hamster brain correlates with regional pathology and scrapie infectivity. Neurology **41:**1482–1490.
23. **Kim, E.-S., H. Li, P. F. McCulloch, L. A. Morrison, K.-W. Yoon, and X. M. Xu.** 2000. Spatial and temporal patterns of transneuronal labeling in CNS neurons after injection of pseudorabies virus into the sciatic nerve of adult rats. Brain Res. **857:**41–55.
24. **Kimberlin, R. H., H. J. Field, and C. A. Walker.** 1983. Pathogenesis of mouse scrapie: evidence for spread of infection from central to peripheral nervous system. J. Gen. Virol. **64:**713–716.
25. **Kimberlin, R. H., S. M. Hall, and C. A. Walker.** 1983. Pathogenesis of mouse scrapie. Evidence for direct neural spread of infection to the CNS after injection of sciatic nerve. J. Neurol. Sci. **61:**315–325.
26. **Kimberlin, R. H., and C. A. Walker.** 1979. Pathogenesis of mouse scrapie: dynamics of agent replication in spleen, spinal cord and brain after infection by different routes. J. Comp. Pathol. **89:**551–562.
27. **Kimberlin, R. H., and C. A. Walker.** 1982. Pathogenesis of mouse scrapie: patterns of agent replication in different parts of the CNS following intraperitoneal infection. J. R. Soc. Med. **75:**618–624.
28. **Kimberlin, R. H., and C. A. Walker.** 1986. Pathogenesis of scrapie (strain 263K) in hamsters infected intracerebrally, intraperitoneally or intraocularly. J. Gen. Virol. **67:**255–263.
29. **Kitamoto, T., T. Muramoto, S. Mohri, K. Doh-Ura, and J. Tateishi.** 1991. Abnormal isoform of prion protein accumulates in follicular dendritic cells in mice with Creutzfeldt-Jakob disease. J. Virol. **65:**6292–6295.
30. **Kuang, R. Z., and K. Kalil.** 1990. Branching patterns of corticospinal axon arbors in the rodent. J. Comp. Neurol. **292:**585–598.
31. **Kucera, P., M. Dolivo, P. Coulon, and A. Flamand.** 1985. Pathways of the early propagation of virulent and avirulent rabies strains from the eye to the brain. J. Virol. **55:**158–162.
32. **Leong, S. K., J. Y. Shieh, and W. C. Wong.** 1984. Localizing spinal-cord-projecting neurons in adult albino rats. J. Comp. Neurol. **228:**1–17.
33. **Lycke, E., K. Kristensson, B. Svennerholm, A. Vahlne, and R. Ziegler.** 1984. Uptake and transport of herpes simplex virus in neurites of rat dorsal root ganglia cells in culture. J. Gen. Virol. **65:**55–64.
34. **Lycke, E., and H. Tsiang.** 1987. Rabies virus infection of cultured rat sensory neurons. J. Virol. **61:**2733–2741.
35. **Mabbott, N. A., F. Mackay, F. Minns, and M. E. Bruce.** 2000. Temporary inactivation of follicular dendritic cells delays neuroinvasion of scrapie. Nat. Med. **6:**719–720.
36. **Manuelidis, L., I. Zaitsev, P. Koni, Z. Y. Lu, R. A. Flavell, and W. Fritch.** 2000. Follicular dendritic cells and dissemination of Creutzfeldt-Jakob disease. J. Virol. **74:**8614–8622.
37. **McBride, P. A., and M. Beekes.** 1999. Pathological PrP is abundant in sympathetic and sensory ganglia of hamsters fed with scrapie. Neurosci. Lett. **265:**135–138.
38. **McBride, P. A., P. Eikelenboom, G. Kraal, H. Fraser, and M. E. Bruce.** 1992.

PrP protein is associated with follicular dendritic cells of spleens and lymph nodes in uninfected and scrapie-infected mice. J. Pathol. **168:**413–418.
39. **McBride, P. A., W. J. Schulz-Schaeffer, M. Donaldson, M. E. Bruce, H. Diringer, H. A. Kretzschmar, and M. Beekes.** 2001. Early spread of scrapie from the gastrointestinal tract to the central nervous system involves autonomic fibers of the splanchnic and vagus nerves. J. Virol. **75:**9320–9327.
40. **McHattie, S., G. A. Wells, J. Bee, and N. Edington.** 1999. Clusterin in bovine spongiform encephalopathy (BSE). J. Comp. Pathol. **121:**159–171.
41. **Montrasio, F., R. Frigg, M. Glatzel, M. A. Klein, F. Mackay, A. Aguzzi, and C. Weissmann.** 2000. Impaired prion replication in spleens of mice lacking functional follicular dendritic cells. Science **288:**1257–1259.
42. **Morin, L. P., and R. I. Wood.** 2001. A stereotaxic atlas of the golden hamster brain. Academic Press, San Diego, Calif.
42a. **National Research Council.** 1996. Guide for the care and use of laboratory animals. National Academy Press, Washington, D.C.
43. **Paxinos, G., and C. Watson.** 1986. The rat brain in stereotaxic coordinates. Academic Press, San Diego, Calif.
44. **Race, R., M. Oldstone, and B. Chesebro.** 2000. Entry versus blockade of brain infection following oral or intraperitoneal scrapie administration: role of prion protein expression in peripheral nerves and spleen. J. Virol. **74:**828–833.
45. **Shamboul, K. M.** 1980. Lumbosacral predominance of vestibulospinal fibre projection in the rat. J. Comp. Neurol. **192:**519–530.
46. **Shieh, J. Y., S. K. Leong, and W. C. Wong.** 1983. Origin of the rubrospinal tract in neonatal, developing and mature rats. J. Comp. Neurol. **214:**79–86.
47. **Strominger, R. N., J. E. McGiffen, and N. L. Strominger.** 1987. Morphometric and experimental studies of the red nucleus in the albino rat. Anat. Rec. **219:**420–428.
48. **Sutherland, K., I. A. Goodbrand, J. E. Bell, and J. W. Ironside.** 1996. Objective quantification of prion protein in spinal cords of cases of Creutzfeldt-Jakob disease. Anal. Cell. Pathol. **10:**25–35.
49. **Taraboulos, A., K. Jendroska, D. Serban, S. L. Yang, S. J. DeArmond, and S. B. Prusiner.** 1992. Regional mapping of prion proteins in brain. Proc. Natl. Acad. Sci. USA **89:**7620–7624.
50. **Tsiang, H., E. Lycke, P. E. Ceccaldi, A. Ermine, and X. Hirardot.** 1989. The anterograde transport of rabies virus in rat sensory dorsal root ganglia neurons. J. Gen. Virol. **70:**2075–2085.
51. **Tyler, K. L., D. A. McPhee, and B. N. Fields.** 1986. Distinct pathways of viral spread in the host determined by reovirus S1 gene segment. Science **233:**770–774.
52. **Ugolini, G., H. G. J. M. Kuypers, and P. L. Strick.** 1989. Transneuronal transfer of herpes virus from peripheral nerves to cortex and brainstem. Science **243:**89–91.
53. **van Keulen, L. J., B. E. Schreuder, R. H. Meloen, G. Mooij-Harkes, M. E. Vromans, and J. P. Langeveld.** 1996. Immunohistochemical detection of prion protein in lymphoid tissues of sheep with natural scrapie. J. Clin. Microbiol. **34:**1228–1231.
54. **van Keulen, L. J., B. E. Schreuder, M. E. Vromans, J. P. Langeveld, and M. A. Smits.** 1999. Scrapie-associated prion protein in the gastrointestinal tract of sheep with natural scrapie. J. Comp. Pathol. **121:**55–63.
55. **Wells, G. A., S. A. Hawkins, R. B. Green, A. R. Austin, I. Dexter, Y. I. Spencer, M. J. Chaplin, M. J. Stack, and M. Dawson.** 1998. Preliminary observations on the pathogenesis of experimental bovine spongiform encephalopathy (BSE): an update. Vet. Rec. **142:**103–106.
56. **Wise, S. P., E. A. Murray, and J. D. Coulter.** 1979. Somatotopic organization of corticospinal and corticotrigeminal neurons in the rat. Neuroscience **4:**65–78.
57. **Yamada, M., H. Tomimitsu, T. Yokota, H. Tomi, N. Sunohara, M. Mukoyama, Y. Itoh, N. Suematsu, E. Otomo, R. Okeda, M. Matsushita, and H. Mizusawa.** 1999. Involvement of the spinal posterior horn in Gerstmann-Straussler-Scheinker disease (PrP P102L). Neurology **52:**260–265.
58. **Zemanick, M. C., P. L. Strick, and R. D. Dix.** 1991. Direction of transneuronal transport of herpes simplex virus 1 in the primate motor system is strain-dependent. Proc. Natl. Acad. Sci. USA **88:**8048–8051.